PB89-124432

Model for Deep Catalytic Oxidation of Hydrocarbon Mixtures in the Strong Pore Diffusion Region

Research Triangle Inst.
Research Triangle Park, NC

Prepared for

Environmental Protection Agency
Research Triangle Park, NC

1988

U.S. Department of Commerce
National Technical Information Service

TECHNICAL REPORT DATA
(Please read Instructions on the reverse before completing)

1. REPORT NO. EPA/600/D-88/237	2.
3. RE[illegible] PB89-124432	
4. TITLE AND SUBTITLE: A Model for Deep Catalytic Oxidation of Hydrocarbon Mixtures in the Strong Pore Diffusion Region	5. REPORT DATE: 1988
	6. PERFORMING ORGANIZATION CODE
7. AUTHOR(S): S.K. Gangwal and T.N. Rogers	8. PERFORMING ORGANIZATION REPORT NO.
9. PERFORMING ORGANIZATION NAME AND ADDRESS: Research Triangle Institute, P.O. Box 12194, Research Triangle Park, North Carolina 27709	10. PROGRAM ELEMENT NO.
	11. CONTRACT/GRANT NO.: CR812522-01-0*
12. SPONSORING AGENCY NAME AND ADDRESS: EPA, Office of Research and Development*, Air and Energy Engineering Research Laboratory, Research Triangle Park, NC 27711	13. TYPE OF REPORT AND PERIOD COVERED: Published paper; 6/85 - 4/87
	14. SPONSORING AGENCY CODE: EPA/600/13

15. SUPPLEMENTARY NOTES: AEERL project officer is Michael Kosusko, Mail Drop 62B, 919/541-2734. In: Catalysis 1987, 38:671-681, 1988

16. ABSTRACT: The paper describes a model for deep catalytic oxidation of hydrocarbon mixtures in the strong pore diffusion region. A laboratory-scale tubular catalytic reactor, used for low-temperature (160-360 C) deep catalytic oxidation of n-hexane and benzene as single components and in a binary mixture, was modeled both with and without internal (pore) diffusion effects. A multicomponent extension on the Mars/van Krevelen mechanism provided the kinetic basis for the reactor models. Experimental conversion data for a 0.1% Pt, 3% Ni/gamma-Al2O3 catalyst, using 120 x 170 mesh particles, were compared to model predictions. Both models provided similar predictions of the single component results indicating the absence of pore diffusion effects in the 120 x 170 mesh particles. Benzene oxidation in the binary mixture was somewhat overpredicted throughout the temperature range, indicating the need for a more rigorous kinetic mechanism. Single component n-hexane oxidation was overpredicted above 260 C, presumably due to external diffusion effects in the laboratory reactor.

17. KEY WORDS AND DOCUMENT ANALYSIS

a. DESCRIPTORS		b. IDENTIFIERS/OPEN ENDED TERMS	c. COSATI Field/Group	
Pollution	Benzene	Pollution Control	13B	
Mathematical Models	Kinetics	Stationary Sources	12A	20K
Hydrocarbons		Catalytic Oxidation	07C	
Oxidation		n-Hexane	07B	
Catalysis			07D	
Hexanes				

18. DISTRIBUTION STATEMENT: Release to Public	19. SECURITY CLASS (This Report): Unclassified	21. NO. OF PAGES: 14
	20. SECURITY CLASS (This page): Unclassified	22. PRICE: PC $13.95/MF $6.95

EPA Form 2220-1 (9-73)

REPRODUCED BY
U.S. DEPARTMENT OF COMMERCE
NATIONAL TECHNICAL INFORMATION SERVICE
SPRINGFIELD, VA. 22161

NOTICE

This document has been reviewed in accordance with U.S. Environmental Protection Agency policy and approved for publication. Mention of trade names or commercial products does not constitute endorsement or recommendation for use.

EPA/600/D-88/237

J.W. Ward (Editor), *Catalysis 1987* 671
© 1988 Elsevier Science Publishers B.V., Amsterdam — Printed in The Netherlands

A MODEL FOR DEEP CATALYTIC OXIDATION OF HYDROCARBON MIXTURES IN THE STRONG PORE DIFFUSION REGION

S. K. Gangwal* and T. N. Rogers, Research Triangle Institute, P.O. Box 12194, Research Triangle Park, N.C. 27709

ABSTRACT

A laboratory-scale tubular catalytic reactor used for low-temperature (160-360 °C) deep catalytic oxidation of n-hexane and benzene as single components and in a binary mixture was modeled both with and without internal (pore) diffusion effects. A multicomponent extension of the Mars/van Krevelen mechanism (ref. 1, ref. 2) provided the kinetic basis for the reactor models. Experimental conversion data for a 0.1-percent Pt, 3-percent Ni/γ-Al_2O_3 catalyst, using 120 x 170 mesh particles, were compared to model predictions. Both models provided similar predictions of the single component results indicating the absence of pore diffusion effects in the 120 x 170 mesh particles. Benzene oxidation in the binary mixture was somewhat overpredicted throughout the temperature range indicating the need for a more rigorous kinetic mechanism. Single component n-hexane oxidation was overpredicted above 260 °C presumably due to external diffusion effects in the laboratory reactor.

INTRODUCTION

In a previous study by Gangwal et al. (ref. 2), a fundamental investigation was performed of low-temperature deep oxidation of n-hexane and benzene over a 120 x 170 mesh, 0.1-percent Pt, 3-percent Ni/γ-Al_2O_3 catalyst under isothermal conditions. These compounds were subjected to oxidation in air as single components and as a binary mixture at temperatures ranging from 160 to 360 °C, weight hourly space velocities (WHSV) ranging from 50 to 1,000, and concentrations ranging from 10 to 600 ppmv. A laboratory-scale system was operated in both integral (high conversion) and differential (less than 10-percent conversion) modes to provide the data necessary.

Significant inhibitions were observed for both benzene and n-hexane oxidation in the binary mixture. An approach based on the Mars/van Krevelen mechanism (ref. 1, ref. 2) was used to explain the results. Mars/van Krevelen kinetic parameters were developed for the individual compounds based on single-component differential reactor data. These kinetic parameters were then incorporated into a proposed multicomponent Mars/van Krevelen rate mechanism (ref. 2) to obtain a kinetic equation for deep oxidation of individual hydrocarbons in a multicomponent mixture:

---

*To whom correspondence should be addressed.

$$r_i = \frac{k_{o_i} k_i C_o C_i}{k_{o_i} C_o + \sum_{j=1}^{n} \frac{k_{o_i}}{k_{o_j}} \eta_j k_j C_j} \quad , i = 1,2.... \qquad (1)$$

The application of Equation (1) to predict integral reactor experimental data indicated a need for a reactor model incorporating diffusional effects. The objective of this paper is to develop and present a solution method for a tubular reactor model incorporating Equation (1) in the strong pore diffusion region under isothermal conditions.

EXPERIMENTAL

Experimental apparatus, conditions, and procedure were described in detail in the previous paper (ref. 2). Properties of the catalyst needed for model development are shown in Table 1. The catalyst was a commercial designation (G-43) obtained from United Catalyst, Inc., Louisville, Kentucky. The constants for n-hexane and benzene for incorporation into Equation (1) were obtained earlier (ref. 2) and are summarized in Table 2.

TABLE 1. CATALYST PHYSICAL PROPERTIES

Pore size range (nm)	Pore volume contained (cm^3/g)
1.4 - 2.9	0.03
2.9 - 14	0.24
14 - 80	0.00
80 - 150	0.08
Total Pore Volume =	0.35 cm^3/g

Particle Density, ρ_p = 1.46 g/cm^3

Surface Area = 210 m^2/g

Micropore Void Fraction = 0.394

Macropore Void Fraction = 0.117

Average Micropore Radius = 2.57 nm

Average Macropore Radius = 57.5 nm

TABLE 2. MARS/VAN KREVELEN RATE EQUATION PARAMETERS

$$r_1 = \frac{k_{o_1} k_1 C_o C_1}{k_{o_1} C_o + \gamma_1 k_1 C_1} \qquad (2)$$

	k_{o_1}, $\left[\frac{cm^3}{g \cdot s}\right]$	k_1, $\left[\frac{cm^3}{g \cdot s}\right]$	γ_1 (--)
n-Hexane	$1.75 \cdot 10^8 \exp[-77{,}905/R_G T]$	$1.66 \cdot 10^{10} \exp[-82{,}763/R_G T]$	9.5
Benzene	$3.41 \cdot 10^{10} \exp[-97{,}939/R_G T]$	$5.347 \cdot 10^{13} \exp[-96{,}351/R_G T]$	7.5

MODEL DEVELOPMENT

Reactor Equations with Internal Diffusion

In this section, the application of the multicomponent intrinsic kinetic rate expression (Equation 1) to the specific reactor and catalyst used in the oxidation experiments is described. The ultimate objective was to develop a reactor model that can predict the kinetic behavior observed experimentally.

Because a tubular reactor is used, at high conversions typical of higher temperatures, the concentrations of the hydrocarbon species change considerably along the reactor length. Thus the kinetic rate of reaction changes along the bed, and a differential equation is needed to describe the reactor concentration profile as a function of catalyst bed depth (or catalyst weight). A possible complication is diffusional mass transfer resistance in the catalyst porous structure at high temperatures. Typically, this would result in a global rate of reaction that is slower than the kinetic rate. In such a case, at any position along the reactor bed, a concentration profile would exist within the catalyst particles themselves, and this would give rise to an intraparticle differential equation for concentration as a function of particle radius. The reactor differential equation and the particle differential equation are coupled through a concentration boundary condition at the external surface of the catalyst particle.

Two types of boundary conditions may be considered. It may be assumed that the mass transfer across the gas film around the particle is equal to the diffusive flux into the particle:

$$-D_{eff(1)} \left[\frac{dc_{1k}}{dR}\right]_{R_o} = k_{f(1)} (C_1 - C_{1k}) \qquad (3)$$

TABLE 2. MARS/VAN KREVELEN RATE EQUATION PARAMETERS

$$r_i = \frac{k_{o_i} k_i C_o C_i}{k_{o_i} C_o + \gamma_i k_i C_i} \qquad (2)$$

	k_{o_i}, $\left[\frac{cm^3}{g \cdot s}\right]$	k_i, $\left[\frac{cm^3}{g \cdot s}\right]$	γ_i (--)
n-Hexane	$1.75 \cdot 10^8 \exp[-77{,}905/R_G T]$	$1.66 \cdot 10^{10} \exp[-82{,}763/R_G T]$	9.5
Benzene	$3.41 \cdot 10^{10} \exp[-97{,}939/R_G T]$	$5.347 \cdot 10^{13} \exp[-96{,}351/R_G T]$	7.5

MODEL DEVELOPMENT

Reactor Equations with Internal Diffusion

In this section, the application of the multicomponent intrinsic kinetic rate expression (Equation 1) to the specific reactor and catalyst used in the oxidation experiments is described. The ultimate objective was to develop a reactor model that can predict the kinetic behavior observed experimentally.

Because a tubular reactor is used, at high conversions typical of higher temperatures, the concentrations of the hydrocarbon species change considerably along the reactor length. Thus the kinetic rate of reaction changes along the bed, and a differential equation is needed to describe the reactor concentration profile as a function of catalyst bed depth (or catalyst weight). A possible complication is diffusional mass transfer resistance in the catalyst porous structure at high temperatures. Typically, this would result in a global rate of reaction that is slower than the kinetic rate. In such a case, at any position along the reactor bed, a concentration profile would exist within the catalyst particles themselves, and this would give rise to an intraparticle differential equation for concentration as a function of particle radius. The reactor differential equation and the particle differential equation are coupled through a concentration boundary condition at the external surface of the catalyst particle.

Two types of boundary conditions may be considered. It may be assumed that the mass transfer across the gas film around the particle is equal to the diffusive flux into the particle:

$$-D_{eff(i)} \left[\frac{dc_{ik}}{dR}\right] \Bigg|_{R_o} = k_{f(i)} (C_i - C_{ik}) \qquad (3)$$

or the external mass transfer resistance may be neglected:

$$C_i \Big|_{R_o} = C_{ik} \Big|_{R_o} \tag{4}$$

In the model development described below, the external mass transfer resistance has been neglected. The reactor model equations for an n-component hydrocarbon mixture are presented in Table 3. These equations have been obtained by a mole balance of species i for a differential section of the bed (reactor equations) and for a differential section within the catalyst particle (particle equations). For simplicity, the model equations were re-written and used in non-dimensional form as shown in Table 4.

TABLE 3. MULTICOMPONENT OXIDATION MODEL WITH INTERNAL DIFFUSION

Reactor Equations ($i = 1,2,3....$)

$$\frac{dC_i}{dW} = \frac{3D_{eff}}{vR_o\rho_p} \left.\frac{dC_{ik}}{dR}\right|_{R_o} \tag{5}$$

Inlet conditions: $C_i\,(0) = C_{io}$ (6)

Particle Equations ($i = 1,2,3...$)

$$\frac{d^2C_{ik}}{dR^2} + \frac{2}{R}\frac{dC_{ik}}{dR} = \frac{(-r_{ik})\,\rho_p}{D_{eff(i)}} \tag{7}$$

Boundary conditions:

$$C_{ik} \Big|_{R_o} = C_i \Big|_{R_o} \tag{8}$$

$$\left.\frac{dC_{ik}}{dR}\right|_0 = 0$$

where r_{ik} is given by Equation (1), the subscript i represents the hydrocarbon species, and the subscript k represents conditions within the particle.

TABLE 4. MULTICOMPONENT OXIDATION MODEL IN NON-DIMENSIONAL FORM

Reactor Equations (i = 1,2,3...)

$$\frac{da_i}{dw} = \lambda_i \left.\frac{da_{ik}}{d\eta}\right|_1 \tag{9}$$

Inlet conditions: $a_i\,(0) = 1$ (10)

Particle Equations (i = 1,2,3...)

$$\frac{d^2a_{ik}}{d\eta^2} + \frac{2}{\eta}\frac{da_{ik}}{d\eta} = h_i^2 \left[\frac{a_{ik}^n}{1 + \sum_{i=1} K_i a_{ik}}\right] \tag{11}$$

Boundary conditions: $a_{ik}\Big|_1 = a_i$ (12)

$$\left.\frac{da_{ik}}{d\eta}\right|_0 = 0 \tag{13}$$

Pore Diffusion Model Assumptions

The assumptions made in the development of the equations in Tables 3 and 4 are:

(1) the tubular reactor flow hydrodynamics may be approximated by plug-flow behavior.
(2) the external mass transfer resistance is negligible.
(3) the particles are spherical with center symmetry.
(4) the reactor is isothermal and the change in volumetric flow rate due to reaction is negligible.

Model Parameters

To properly account for pore diffusion effects, the effective diffusivity, $D_{eff(i)}$, must be estimated for each hydrocarbon species. This parameter is a function of both the hydrocarbon type and the complex porous structure of the catalyst. The catalyst used (G-43, United Catalyst, Inc.) has a bimodal pore size distribution (see Table 1). The random pore model proposed by Wakao and Smith (ref. 3) was used to estimated $D_{eff(i)}$ for each hydrocarbon species as a function of temperature for use in the numerical solution. All other parameters were known from experimental measurements (Table 2) and the catalyst properties

in Table 1. The catalyst amount in the reactor was 17 mg and the volumetric flow rate corresponding to a WHSV of 209 was 45.8 cm^3/min (referred to 0 °C and 0.1 MPa) for the integral reactor experiments. The inlet concentration of benzene was 375 ppmv in the single component gas and 189 ppmv in the binary mixture. The corresponding values for n-hexane were 410 ppmv and 190 ppmv.

Solution Procedure

To solve the non-dimensional reactor equations, the second-order particle differential equation was first converted into two first-order differential equations. Equations (11) through (13) were rewritten as:

$$\frac{da_{ik}}{d\eta} = m_i \quad , (i = 1,2,3...) \tag{14}$$

$$\frac{dm_i}{d\eta} + \frac{2m_i}{\eta} = h_i^2 \left[\frac{a_{ik}}{1 + \sum_{i=1}^{n} K_i a_{ik}} \right] \quad , (i = 1,2,3...) \tag{15}$$

With boundary conditions:

$$a_{ik} \Big|_1 = a_i \quad , (i = 1,2,3...) \tag{16}$$

$$\text{and } m_i \Big|_0 = 0 \quad , (i = 1,2,3...) \tag{17}$$

A numerical method is required to solve simultaneously the resulting coupled first-order differential equations. The primary difficulty in using a straightforward Runge-Kutta method is that the concentration at the center of the particle is unknown. An initial condition required to advance the Runge-Kutta iteration is therefore not available.

This difficulty was overcome by a trial-and-error technique. First, the catalyst bed was divided into a number of segments of equal length and catalyst content. In a given segment (i.e., at a given position in the catalyst bed), the particle equations were then solved. The solution method was a combination of a sixth-order Runge-Kutta-Verner method (IMSL routine DVERK) and a global constrained function minimizer (IMSL routine ZXMWD) using an IBM 370 mainframe computer. To start the iterative process, a guess value was assigned at the particle center for each hydrocarbon species concentration. Next, the Runge-Kutta procedure was employed to determine the species concentrations at the external particle surface, and these values were then compared to the bulk gas

concentrations in the reactor segment. Adjustment of the particle center concentrations (by the IMSL routine ZXMWD) was used to minimize this concentration difference. The objective function was the sum of the squares of the dimensionless concentration differences of the various species. The dimensionless concentration gradient (m_i) at the catalyst surface was obtained and substituted in Equation (9) to calculate the bulk gas-phase species concentration gradient which in turn was used to obtain gas-phase concentrations in the next reactor segment. This series of operations was repeated sequentially in the reactor, segment after segment from the bed inlet, until the concentration profiles in the bed were determined completely. In practice, little accuracy advantage was observed when the number of reactor segments was increased beyond the value of 20 chosen in this study.

Reactor Equations Without Diffusional Resistance

For comparison purposes with the pore diffusion reactor model, the simpler case was also considered where internal diffusional resistances are neglected. In this special case, the particle equation is not considered and the reactor equation reduces to:

$$\frac{dC_i}{dW} = \frac{(-r_i)}{v} \quad , \quad (i = 1,2,3\ldots) \tag{18}$$

$$\text{with inlet conditions } C_i\ (0) = C_{io}, \quad (i = 1,2,3\ldots) \tag{19}$$

This reactor model represents a simple isothermal plug flow reactor with a kinetic rate of reaction based on the multicomponent Mars/van Krevelen mechanism (ref. 2).

In dimensionless form, Equations (18) and (19) may be written as:

$$\frac{da_i}{dw} = \beta \frac{a_i}{1 + \sum_{i=1}^{n} K_i a_i} \quad , \quad (i = 1,2,3\ldots) \tag{20}$$

$$a_i\ (0) = 1, \quad (i = 1,2,3\ldots) \tag{21}$$

The fractional conversion of the ith species is defined as:

$$f_i = 1 - \frac{C_i}{C_{io}} = 1 - a_i \tag{22}$$

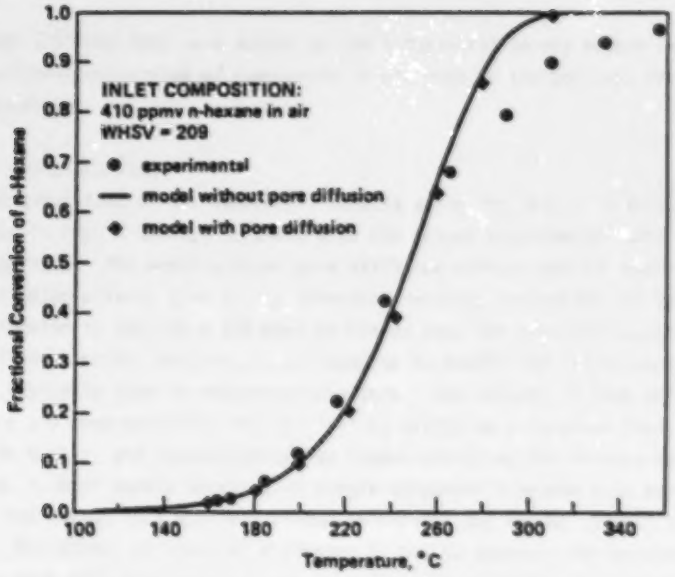

Fig. 1. Comparison of model predictions and experimental data for n-hexane conversion as a single component.

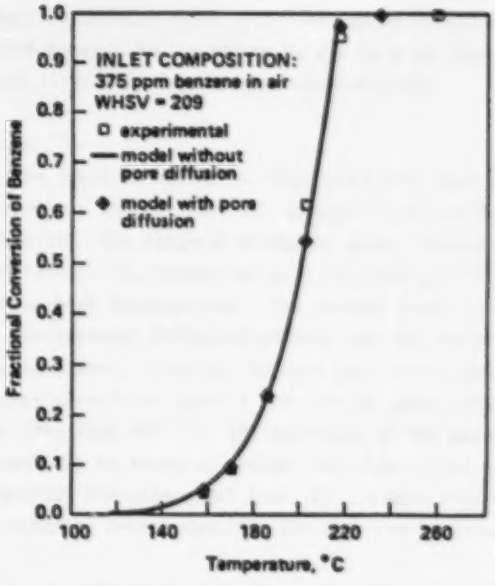

Fig. 2. Comparison of model predictions and experimental data for benzene conversion as a single component.

Equations (20) and (21) were solved by the Runge-Kutta-Verner method to obtain the fractional conversion of components in mixtures at the bed exit for a series of temperatures.

RESULTS AND DISCUSSION

The simulation of the laboratory results using the reactor models developed are shown in Fig. 1 through 3, along with the actual experimental data (ref. 2) for comparison. The model without pore diffusion effects and the model with pore diffusion effects give nearly identical results, indicating the absence of pore diffusion in the 120 x 170 mesh particles used for the experiments. The pore diffusion model, however, is believed to be useful for larger particles (~6 mm) typically used in industrial reactors. The absence of pore diffusion in the 120 x 170 mesh particles was verified by assigning a range of reasonable values to $D_{eff(i)}$ and demonstrating the insensitivity of the results to $D_{eff(i)}$. From Fig. 1, both models overpredict single component n-hexane data above about 260 °C, indicating that external diffusion effects may become significant above 260 °C. The effect of external diffusion is not so apparent for benzene (Fig. 2). The pore diffusion model is somewhat superior at higher conversions than the simple reactor model without internal diffusion. From Fig. 3, the benzene data in the mixture is overpredicted throughout the temperature range, confirming the need for a larger adsorption term for benzene in the kinetic equation, as concluded previously (ref. 2). The overprediction of n-hexane conversion in the mixture between 200 to 260 °C is due to a smaller adsorption term for n-hexane resulting from the benzene overprediction.

CONCLUSIONS

For the catalyst mesh size range (120-170) examined experimentally (ref. 2), the modeling results indicate no significant oxidation inhibition due to pore diffusion. The internal diffusion model, however, would no doubt yield different results for industrial-size catalyst particles where pore diffusion dominates at high temperatures. The reactor model should be extended to account for probable external diffusion effects causing overprediction of conversions at higher temperatures. Finally, because the reactor model overpredicts the mixture benzene conversion even in the kinetic-controlled region (e.g., for temperatures less than 200 °C), the magnitude of the model's adsorption term for benzene needs to be somewhat greater than that given by the proposed multicomponent Mars/van Krevelen model (ref. 2). A more rigorous kinetic representation is thus needed to better describe the observed benzene behavior.

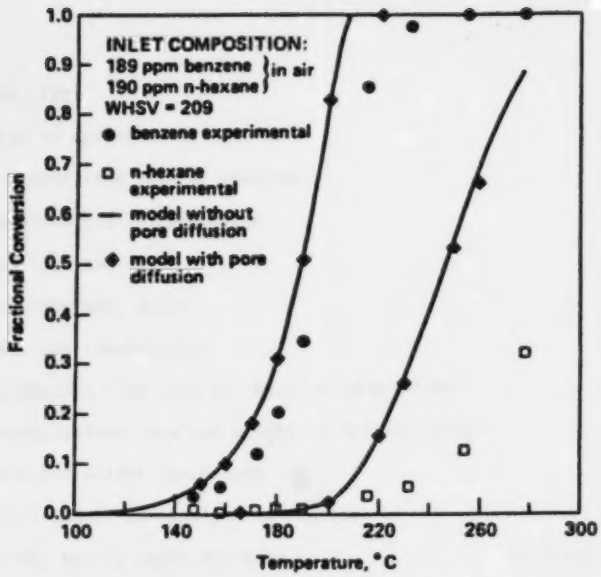

Fig. 3. Comparison of model predictions and experimental data for binary benzene/n-hexane mixture.

NOMENCLATURE

		Units
C_i	= gas-phase hydrocarbon [VOC] concentration	[mol/cm^3]
C_{ik}	= intraparticle concentration of species i	[mol/cm^3]
C_{io}	= inlet hydrocarbon [VOC] concentration	[mol/cm^3]
C_o	= oxygen concentration	[mol/cm^3]
$D_{eff(i)}$	= effective diffusivity of species i	[cm^2/s]
f_i	= fractional conversion of species i	[--]
h_i	= Thiele modulus for species i, $R_o \sqrt{(k_i \rho_p)/D_{eff(i)}}$	[--]
$k_{f(i)}$	= mass transfer coefficient of species i	[cm/s]
k_i	= surface reduction rate constant for species i	[cm^3/(g•s)]
k_{o_i}	= surface reoxidation rate constant for species i	[cm^3/(g•s)]
K_i	= $\gamma_i (k_i/k_{o_i})(C_{io}/C_o)$	[--]

m_i	= $(d\alpha_{ik}/d\eta)$	[--]
r_i	= rate of oxidation of species i	[mol/(g•s)]
r_{ik}	= intraparticle rate of reaction	[mol/(g•s)]
R	= particle radial coordinate	[cm]
R_o	= particle radius	[cm]
R_G	= gas constant, 8.314	[J/(mol•K)]
T	= absolute temperature	[K]
v	= volumetric flow rate at reaction temperature	[cm^3/s]
w	= dimensionless catalyst weight in reactor, W/W_F	[--]
W	= catalyst weight coordinate	[g]
W_F	= total weight of catalyst in reactor	[g]
WHSV	= weight hourly space velocity	[g gas/g catalyst•h]

Greek Symbols

α_i	= dimensionless gas phase concentration, C_i/C_{io}	[--]
α_{ik}	= dimensionless intraparticle concentration, C_{ik}/C_{io}	[--]
β	= $(k_i \cdot W_F)/v$	[--]
γ_i	= stoichiometric coefficient for deep oxidation of species i	[--]
η	= dimensionless particle radial coordinate, R/R_o	[--]
λ_i	= $(3\ D_{eff(i)}\ W_F)/(vR_o^2\ \rho_p)$	[--]
ρ_p	= particle density	[g/cm^3]

ACKNOWLEDGEMENTS

Financial support for this work was provided by the U.S. Environmental Protection Agency and the U.S. Air Force under Cooperative Agreement No. CR812522-01-0 and Interagency Agreement No. RW57931254. This paper has not been subjected to the EPA's peer review and therefore does not necessarily reflect the views of the Agency and no official endorsement should be inferred.

REFERENCES

1 P. Mars and D. W. van Krevelen, Chem. Eng. Sci., 3(1954), 41.
2 S. K. Gangwal, M. E. Mullins, J. J. Spivey, P. R. Caffrey, and B. A. Tichenor, "Kinetics and Selectivity of Deep Catalytic Oxidation of n-Hexane and Benzene", Applied Catalysis, 36(1988) 231.
3 N. Wakao and J. M. Smith, Chem. Eng. Sci., 17(1962) 825.